Taylor & Francis
Taylor & Francis Group

REPORT

🔓 OPEN ACCESS   Check for updates

A novel anti-NGF PEGylated Fab' provides analgesia with lower risk of adverse effects

Yukari Koya [ID][a], Hirotsugu Tanaka[b], Eiji Yoshimi[a], Nobuaki Takeshita[a], Shuji Morita[a], Hiroki Morio[a], Kanako Mori[a], Hiroshi Fushiki[a], and Masazumi Kamohara[a]

[a]Drug Discovery Research, Astellas Pharma Inc, Tsukuba, Japan; [b]Incubation Lab, Astellas Innovation Management LLC, Cambridge, MA, USA

ABSTRACT

Nerve growth factor (NGF) has emerged as a key driver of pain perception in several chronic pain conditions, including osteoarthritis (OA), and plays an important role in the generation and survival of neurons. Although anti-NGF antibodies improve pain control and physical function in patients with clinical chronic pain conditions, anti-NGF IgGs are associated with safety concerns such as effects on fetal and postnatal development and the risk of rapidly progressive osteoarthritis. To overcome these drawbacks, we generated a novel anti-NGF PEGylated Fab' antibody. The anti-NGF PEGylated Fab' showed specific binding to and biological inhibitory activity against NGF, and analgesic effects in adjuvant-induced arthritis model mice in a similar manner to an anti-NGF IgG. In collagen-induced arthritis model mice, the anti-NGF PEGylated Fab' showed higher accumulation in inflamed foot pads than the anti-NGF IgG. In pregnant rats and non-human primates, the anti-NGF PEGylated Fab' was undetectable in fetuses, while the anti-NGF IgG was detected and caused abnormal postnatal development. The PEGylated Fab' and IgG also differed in their ability to form immune complexes in vitro. Additionally, while both PEGylated Fab' and IgG showed analgesic effects in sodium monoiodoacetate-induced arthritic model rats, their effects on edema were surprisingly quite different. While the anti-NGF IgG promoted edema over time, the anti-NGF PEGylated Fab' did not. The anti-NGF PEGylated Fab' (ASP6294) may thus be a potential therapeutic candidate with lower risk of adverse effects for various diseases in which NGF is involved such as OA and chronic back pain.

Introduction

Osteoarthritis (OA) is the most common form of arthritis and the fastest growing chronic pain disease worldwide.[1] It is characterized by pain, inflammation, and functional disability.[2] Treatment of pain associated with OA is problematic because many standard therapies provide minimal pain relief and do not address the underlying mechanisms driving the disease pathophysiology.[3,4]

Nerve growth factor (NGF) plays important roles in the growth, maintenance, and survival of target neurons.[5] It is also considered a key modulator of pain perception in several chronic pain conditions, including OA.[6–9] The physiological actions of NGF are mediated via the high-affinity tyrosine kinase receptor tropomyosin receptor kinase A (TrkA) and low-affinity NGF receptor p75.[10] Anti-NGF antibodies have been shown to significantly improve pain and physical function in pre-clinical animal models and patients with clinical chronic pain conditions.[11] However, anti-NGF therapeutic antibodies are associated with several safety concerns. First, when the antibodies are administered to women of childbearing potential, they could have adverse effects on fetal and postnatal development. The mutation in the NGF gene or TrkA gene in patients causes congenital insensitivity to pain.[12,13] In addition, studies using NGF and TrkA-deficient mice have demonstrated that deletion of NGF inhibits the development of embryonic sensory and sympathetic neurons.[14,15] These reports suggest that NGF/TrkA signaling is essential for the early stages of neural development. This concern is pertinent as many female patients of childbearing age have NGF-related diseases such as chronic low back pain.[16–18] Second, anti-NGF therapeutic antibodies can increase the risk of developing rapidly progressive osteoarthritis (RPOA). Clinical trials have shown an association with higher doses of tanezumab, a humanized anti-NGF IgG, alone or with non-steroidal anti-inflammatory drugs, although the underlying molecular mechanism remains unknown.[11,19]

Here, we report the development and assessment of a novel anti-NGF PEGylated human Fab' antibody fragment (Fab'-PEG). In most mammalian species, including humans, the transplacental passage for maternal IgG is predominantly mediated by pH-dependent binding to the neonatal Fc receptor, FcRn.[20,21] Unlike IgG, Fab' fragments might be prevented from cross-placental transfer during pregnancy because of the absence of the Fc domain.[22,23] However, given the absence of the Fc domain and the small size of Fab' fragments (about 50 kDa), they can have a short half-life, with rapid removal from the kidneys and blood circulation being inevitable. To overcome this problem, we employed the idea of covalently introducing a branched 40 kDa polyethylene glycol (PEG) into the C-terminal region of the Fab' fragment.[22] PEG is a biocompatible polymer that has been used to enhance pharmacokinetics by reducing renal excretion and to improve

---

localization at specific disease sites, reduce immunogenicity, and increase solubility.[22,24] Several pegylated drugs have been approved by the U.S. Food and Drug Administration, including certolizumab pegol, a PEGylated Fab′ antibody against tumor necrosis factor (TNF)-α.[22] As the half-life of Fab' fragments is known to change depending on the size and number of PEGs added, we selected a branched 40 kDa PEG, which is expected to have a half-life close to that of IgG.[25] In one study of pregnant rats, administration of anti-TNF-α PEGylated Fab' led to undetectable or very low concentrations of the antibody in rat fetuses.[26] Similarly, a case study of 10 women who received certolizumab pegol during pregnancy found that concentrations of certolizumab pegol in infants' blood and in cord blood on the day of birth were undetectable or very low, whereas IgG drugs adalimumab and infliximab crossed the placenta during pregnancy.[22] These reports indicate that PEGylated Fab' fragments are not actively transported across the placenta.

Additionally, unlike whole IgG, Fab' fragments do not induce Fc-mediated effects in complement-dependent cytotoxicity or antibody-dependent cell-mediated cytotoxicity. Moreover, since Fab' fragments only have a monovalent antigen-binding site, they cannot form large immune complexes (ICs) by crosslinking antigens. Antibodies that have two or more antigen-binding sites, such as IgG, and antigens that form multimers can form large ICs, which can cause adverse effects via mechanisms such as platelet aggregation and complement activation. In fact, bevacizumab, an antibody against vascular endothelial growth factor, forms an IC and induces thrombosis via platelet aggregation.[27,28] Since NGF also forms a dimer,[10] anti-NGF antibodies have a risk of adverse effects mediated by IC formation. We hypothesized that the above-mentioned differences in biological activity between anti-NGF Fab'-PEG and IgG affect their safety when used to treat OA. To test this hypothesis, we evaluated our anti-NGF Fab'-PEG in a sodium monoiodoacetate (MIA)-induced arthritis model. The MIA-induced OA model is widely used as a preclinical model of OA because the injection of MIA into the intra-articular space in the knee induces joint degeneration and chronic pain-associated symptoms in rats that mimic aspects of end-stage OA with severe pain.[29–31]

In this report, we propose that anti-NGF Fab'-PEG might be a useful therapeutic drug for OA with strong analgesic effects and fewer safety concerns.

Results

Generation of anti-NGF Fab'-PEG

First, we immunized VelocImmune mice with a recombinant human NGF protein. Using a standard method, lymphocytes from immunized mice were fused with mouse-derived myeloma cells to generate hybridomas that produce anti-NGF antibodies. To select antibodies that bind NGF and inhibit the interaction between NGF and TrkA, competitive ELISA was performed using biotinylated human NGF and recombinant TrkA-Fc protein. Additionally, cross-reactivity to mouse NGF was checked by competitive ELISA using biotinylated mouse NGF. Next, to check binding specificity, we evaluated

binding activity to human neurotrophin-3 (NT-3) by ELISA. NT-3 has the highest homology to NGF in the neurotrophic factor family of proteins. Second, to identify antibodies that inhibit NGF/TrkA cell signaling, we performed an NGF-induced calcium influx assay using TrkA-stably expressing HEK293 cells and a Fluorescent Imaging Plate Reader (FLIPR). Third, to identify a functional antagonistic antibody, we conducted a cell viability assay using PC12 cells expressing endogenous TrkA and p75. Fourth, to select Fab fragments of antibodies possessing inhibition activity, we generated Fabs by papain digestion and evaluated their activity. As a result, we identified an antibody clone with high neutralizing activity even in the Fab form.

Following antibody screening, we generated an anti-NGF Fab'-PEG antibody using both genetic and chemical engineering technologies (Figure 1a). The inhibitory activity of the antibody against NGF/TrkA binding and NGF/TrkA signaling were evaluated by competitive ELISA (Figure 1b), calcium influx assay (Figure 1c) and TrkA phosphorylation assay (Figure 1d). The anti-NGF Fab'-PEG showed concentration-dependent inhibitory effects that were comparable to the anti-NGF IgG in each assay. Next, we evaluated the Fab's binding specificity to four neurotrophins, NGF, brain-derived neurotrophic factor (BDNF), NT-3 and neurotrophin-4 (NT-4), by ELISA (Figure 1e). The anti-NGF Fab'-PEG bound specifically to NGF. We also evaluated cross-reactivity to human, mouse and rat NGF using the Gyrolab system, a recently reported highly sensitive platform for measuring protein–protein interactions.[32] The dissociation constant (K_D) of the anti-NGF Fab'-PEG to human NGF was 11.89 pmol/L (95% confidence interval: 5.77 to 24.51), that to mouse NGF was 12.13 pmol/L (95% confidence interval: 2.78 to 52.95) and that to rat NGF was 21.07 pmol/L (95% confidence interval: 15.42 to 28.81). Anti-NGF Fab'-PEG thus showed similar binding affinities to NGF from each species tested. The systemic pharmacokinetics of single intravenous administration of 0.2 mg/kg of anti-NGF Fab'-PEG or 0.3 mg/kg of anti-NGF IgG in mice were determined based on the plasma concentration-time profile. The half-life of anti-NGF Fab'-PEG was 18.3 ± 2.6 hours (n = 3, mean ± SD), which was slightly shorter but comparable to the half-life of anti-NGF IgG of 21.6 ± 3.4 hours.

Effect of anti-NGF Fab'-PEG on an in vivo arthritis model

First, we evaluated the analgesic effect of the anti-NGF Fab'-PEG on adjuvant-induced arthritis (AIA) model mice. The mice were intravenously administered anti-NGF Fab'-PEG or IgG and injected with an adjuvant into their footpads, and then assessed for the degree of inflammatory pain by measuring the number of rearing events. Treatment with anti-NGF Fab'-PEG significantly reversed the decreased number of rearing events observed in AIA model mice (Figure 2a). The number of such events (mean ± SEM) was as follows: sham 208 ± 30; vehicle 51 ± 16 (P = .0003); anti-NGF Fab'-PEG 0.2 mg/kg 137 ± 14 (P = .0112); anti-NGF Fab'-PEG 0.6 mg/kg, 160 ± 22 (P = .0010). The anti-NGF Fab'-PEG showed comparable analgesic effect to the anti-NGF IgG.

Next, we investigated the tissue distribution of NGF inhibitors in areas of inflammation in a murine model of arthritis.
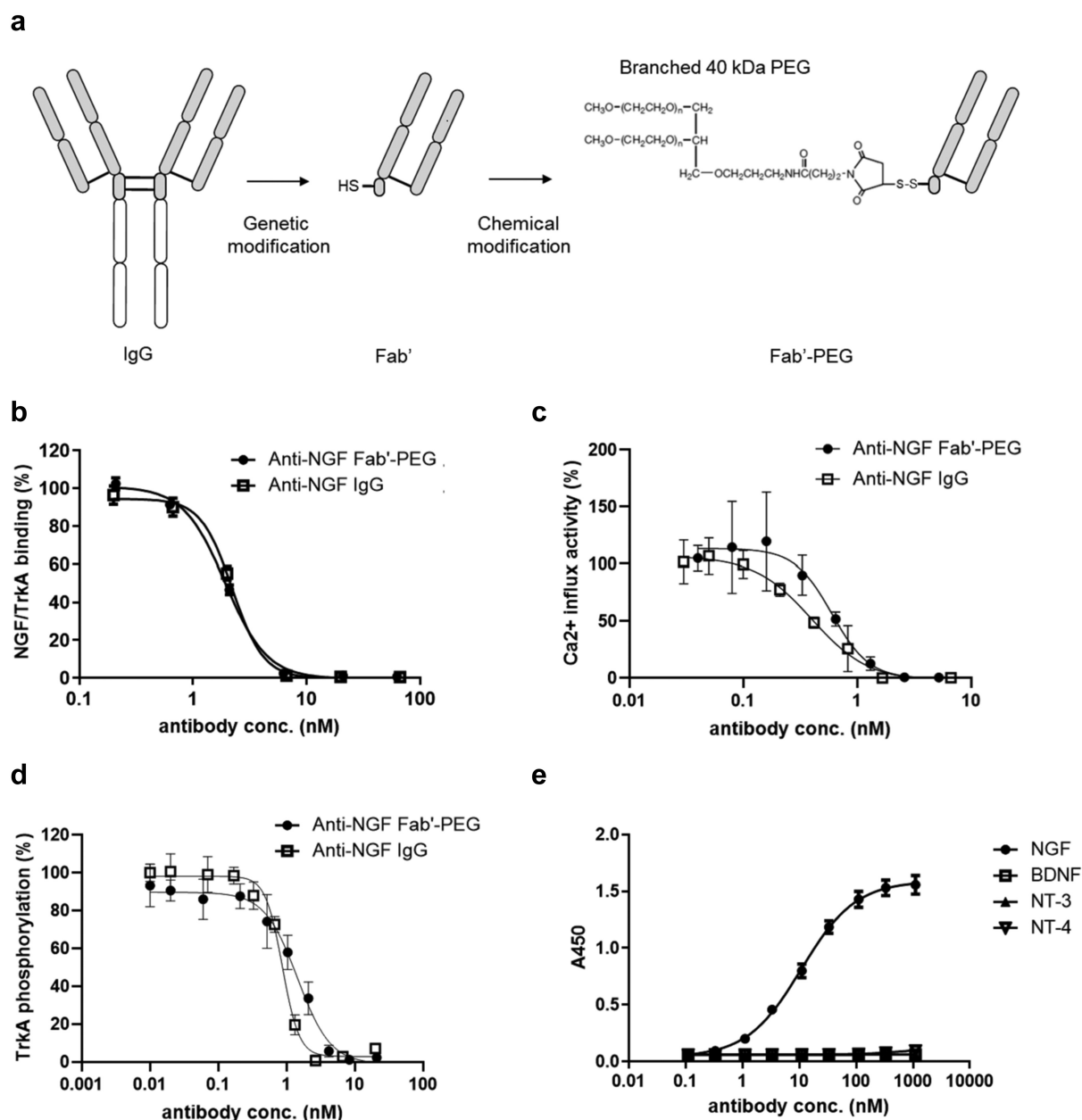
Figure 1. Generation and characterization of a novel anti-NGF Fab'-PEG. (a) Scheme showing how the Fab'-PEG was generated. (b) Inhibitory activity of NGF/TrkA binding in competitive ELISA. (c) The inhibitory activity of NGF induced a calcium influx in TrkA-expressing HEK293 cells. (d) The inhibitory activity of NGF induced TrkA phosphorylation in TrkA-expressing HEK293 cells. Values indicate percent activity, with the effect of NGF alone (without antibody) representing 100%, and the basal activity without NGF or maximum concentration of anti-NGF Fab'-PEG defined as 0%. (e) Binding activity of the anti-NGF Fab'-PEG to human NGF, BDNF, NT-3 and NT-4. Values indicate absorbance at 450 nm. Data are presented as mean ± SD.

A previous study demonstrated that, certolizumab pegol, an anti-TNF-α Fab'-PEG, was more effectively distributed to inflamed arthritic paws than anti-TNF-α IgG.[33] In the present study, we intravenously administered fluorescence-labeled anti-NGF Fab'-PEG or IgG to collagen-induced arthritis (CIA) model mice or normal mice, and analyzed the fluorescence intensity in inflamed arthritic paws for 50 hours after administration using the IVIS Spectrum in vivo imaging system (Figure 2b,c,d). Both anti-NGF Fab'-PEG and IgG were more effectively distributed to the inflamed paws of arthritis mice than paws of normal mice. However, at 2 hours after administration, the level of anti-NGF Fab'-PEG in inflamed arthritic paws compared with normal paws was significantly

greater than that observed for anti-NGF IgG (Figure 2d). Meanwhile, the average footpad thickness was similar between the groups (anti-NGF Fab'-PEG group vs anti-NGF IgG group = 4.42 vs 4.41 mm). The difference in distribution of these antibodies into inflamed tissue may affect their efficacy, tolerability, rapidity, and/or sustainability.

Placental transfer and risk of developmental toxicity

First, we compared the placental transfer efficiency of the anti-NGF Fab'-PEG and IgG in pregnant female rats. Anti-NGF Fab'-PEG or IgG was intravenously administered to dams at
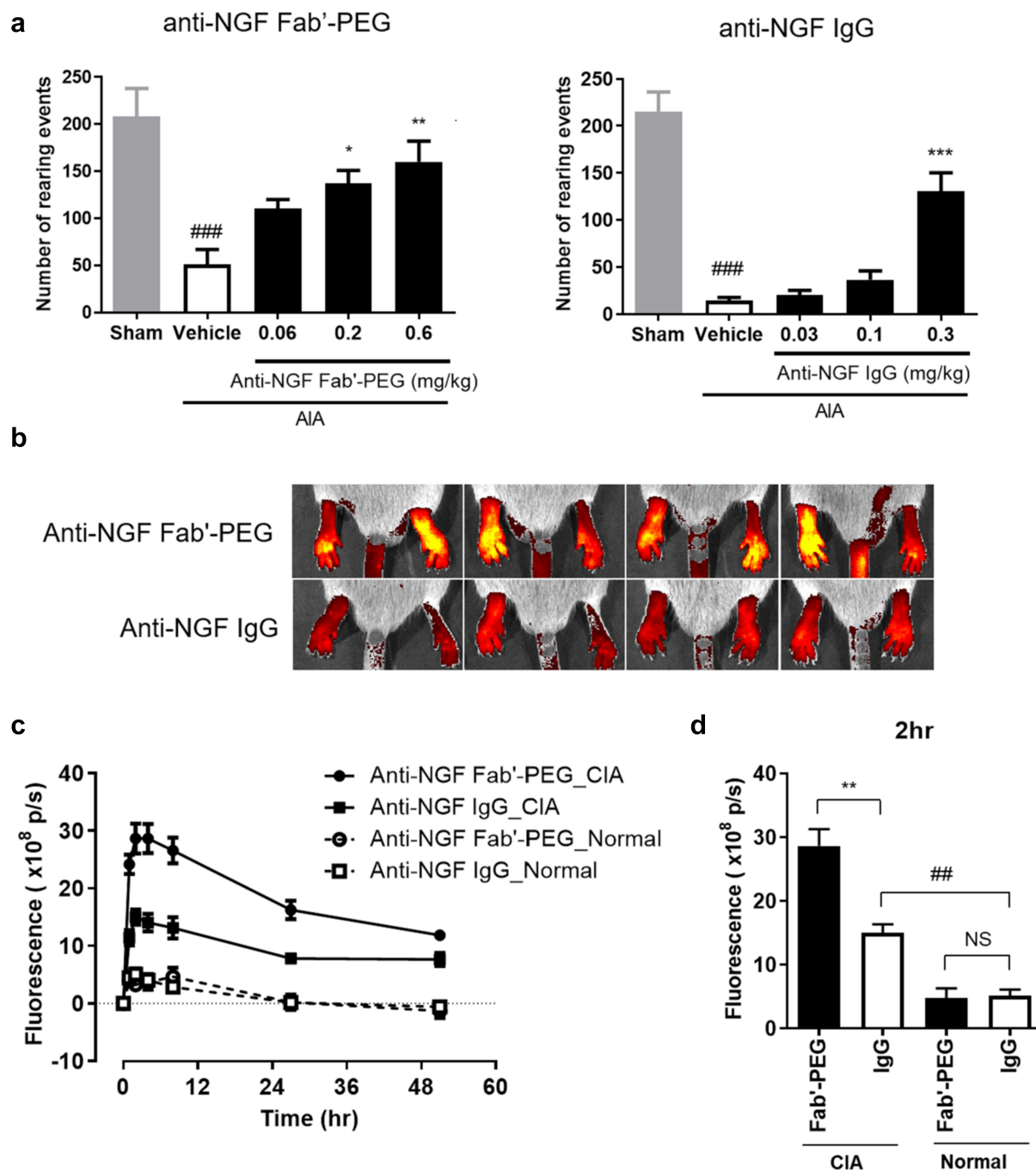
Figure 2. Analgesic effect and distribution of anti-NGF Fab'-PEG in arthritis models. (a) Analgesic effect of the anti-NGF Fab'-PEG and anti-NGF IgG in a murine AIA model. The number of rearing events was measured as an indicator of pain. Data are expressed as the mean ± SEM of 7–8 mice in each group. ### $P < .001$, statistically significant compared to the sham group (Student's t-test). * $P < .05$, ** $P < .01$, *** $P < .001$, statistically significant compared to the vehicle group (Dunnett's multiple comparisons test). (B, C, D) Biofluorescence imaging of the anti-NGF Fab'-PEG and anti-NGF IgG distribution in the inflamed paws of the murine CIA model. The images were captured and analyzed using the IVIS Spectrum in vivo imaging system (B, 2 hours after administration in CIA mice) and the fluorescence intensities were plotted at each time point. Change in fluorescence intensity (c) and fluorescence intensity 2 hours after administration (d). Data are expressed as the mean ± SEM of 4 mice in each group. ## $P < .01$, statistically significant compared to the anti-NGF IgG-Normal group. ** $P < .01$, statistically significant compared to the anti-NGF IgG-CIA group (Student's t-test).

gestational day (GD) 17, and the antibody concentration in plasma was measured at GD 20. As shown in Figure 3a, 75.9% of the concentration of anti-NGF IgG was transferred to fetuses (average plasma concentration in dams and fetuses was 7.1 and 5.4 μg/mL, respectively). In contrast, the plasma concentration of anti-NGF Fab'-PEG was below the limit of quantification (0.01 μg/mL) in all fetuses, despite a plasma concentration of 12.1 μg/mL in dams. This result suggests that the anti-NGF

Fab'-PEG may be prevented from placental transfer during pregnancy in rats.

Next, we evaluated the effects of the anti-NGF Fab'-PEG or IgG on dams and embryo-fetal and postnatal development in rats (Table 1). In dams, while neither antibody caused death or abnormal general signs during the gestation or lactation period, the anti-NGF IgG decreased body weight and food consumption. In pups, neither antibody affected the total number
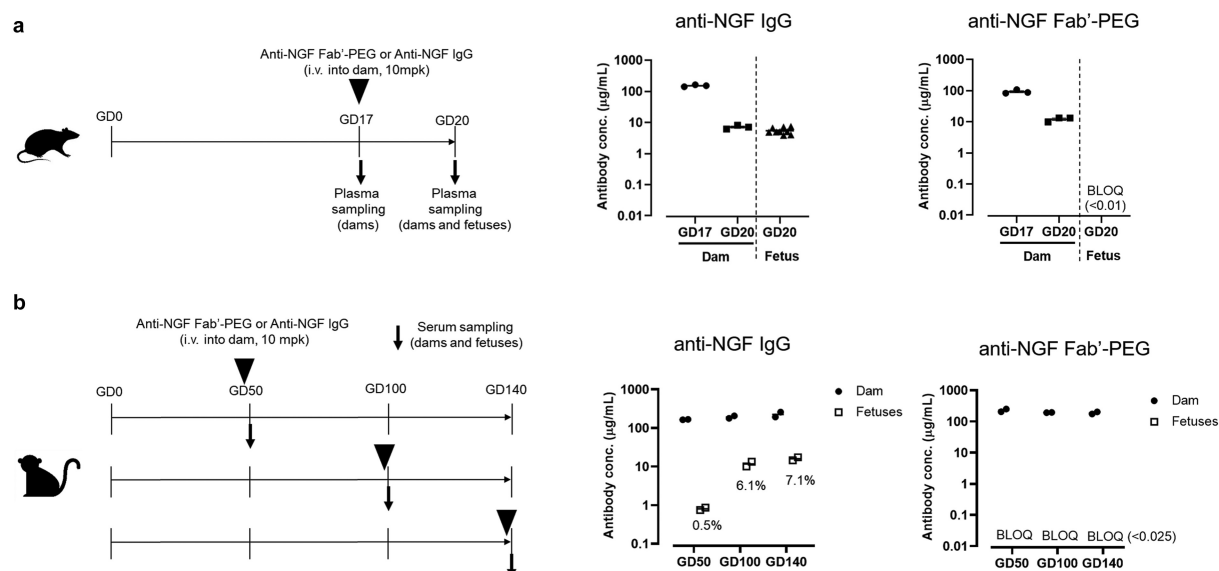
Figure 3. Comparison of placental transfer of anti-NGF Fab'-PEG and anti-NGF IgG in rats and NHPs. (a) Scheme of the study design used to evaluate placental transfer in pregnant rats and the concentration of anti-NGF IgG or anti-NGF Fab'-PEG in plasma from rat dams and fetuses. Data are expressed as individual values and the mean ± SEM of 3 dams or 9 fetuses in each group. (b) Scheme of the study design used to evaluate placental transfer in pregnant cynomolgus monkeys and the concentration of anti-NGF IgG or anti-NGF Fab'-PEG in serum from cynomolgus monkey dams and fetuses. Data are expressed as individual values and the mean of 2 dams or 2 fetuses in each group. % values represent the proportion of the concentration of anti-NGF IgG in fetuses to dams.

Table 1. Effects of the anti-NGF Fab'-PEG or IgG on dams and embryo-fetal and postnatal development in rats.

Drug		Anti-NGF IgG			Anti-NGF Fab'-PEG		
Dose (mg/kg)		10	30	100	3	10	30
Day of dosing			GD7,14			Every 2 days from GD7 to GD19	
Number of dams		5	6	6	6	6	6
F_0 Dams							
Died or sacrificed moribund			(-)			(-)	
General signs			(-)			(-)	
Body weight	Gestation period		(-)			(-)	
	Lactation period		Decrease			(-)	
Food consumption	Gestation period		(-)			(-)	
	Lactation period		Decrease			(-)	
Mean duration of gestation (days)			(-)			(-)	
Abnormal parturition			(-)			(-)	
Gestation index (%)			(-)			(-)	
F_1 Pups							
Total No. of pups delivered (mean)		72 (14.4)	81 (13.5)	80 (13.3)	90 (15.0)	80 (13.3)	82 (13.7)
Total No. of live pups (mean)		72 (14.4)	80 (13.3)	80 (13.3)	88 (14.7)	78 (13.0)	82 (13.7)
Live birth index (%)			(-)			(-)	
No. of pups with milk in stomach			Decrease			(-)	
Body weight			Decrease			(-)	
Viability index at LD 4 (%) [§]		45.7	70.1	86.3	99.1	100	94.9
Weaning index (%) [¶]		0	0	0	100	100	100
General signs	Found dead or cannibalized		Increase			(-)	
	Trauma		Increase			(-)	
Pain response		2/9	0/6	0/8	48/48	48/48	46/46

[§]Viability index (%) = (No. of live pups before cull (LD 4)/No. of pups delivered) × 100
[¶]Weaning index (%) = (No. of live pups at LD 21/No. of live pups after cull (LD 4)) × 100
GD: gestational day, LD: lactation day

of pups delivered, live birth index, mean pup body weight at birth, or pup external abnormalities at birth. However, all pups in the anti-NGF IgG-treated groups showed markedly decreased body weight from Day 4 after birth and died before weaning. These pups lacked milk in their stomachs and exhibited attenuated or failed pain response. In contrast, no anti-NGF Fab'-PEG-related effects were noted on the viability index, weaning index, general signs, suckling ability, body weight gain, macroscopic observation of eyes, pain response,

or external or gross pathological findings in any drug concentration group.

Finally, we investigated the placental transfer of anti-NGF Fab'-PEG and IgG in cynomolgus monkeys during pregnancy. At GD 50, 100 and 140, anti-NGF Fab'-PEG or IgG was intravenously administered to dams and the antibody concentration was measured in dams and fetuses. No dams died, and no abnormalities in clinical signs or body weight were observed in any dam. As shown in Figure 3b, on GD 50, 0.5% of the

concentration of anti-NGF IgG had transferred to the fetuses from dams. On GDs 100 and 140, the concentration of anti-NGF IgG in fetuses was approximately 6% to 7% of those in dams. In contrast, the serum concentration of anti-NGF Fab'-PEG was below the limit of quantification (0.025 μg/mL) in all fetal samples on GD 50, 100, and 140. These results indicate that the anti-NGF Fab'-PEG does not undergo placental transfer in cynomolgus monkeys.

Immune complex formation and knee edema

We first compared the IC-forming ability of the anti-NGF Fab'-PEG and IgG. Each antibody was mixed with NGF at a 1:1 molar ratio. After incubation, the particle size was measured by dynamic light scattering (DLS) analysis using a Zetasizer Nano (Figure 4a and Table 2). In the case of anti-NGF IgG, the peak particle diameter shifted from 8.7 nm to
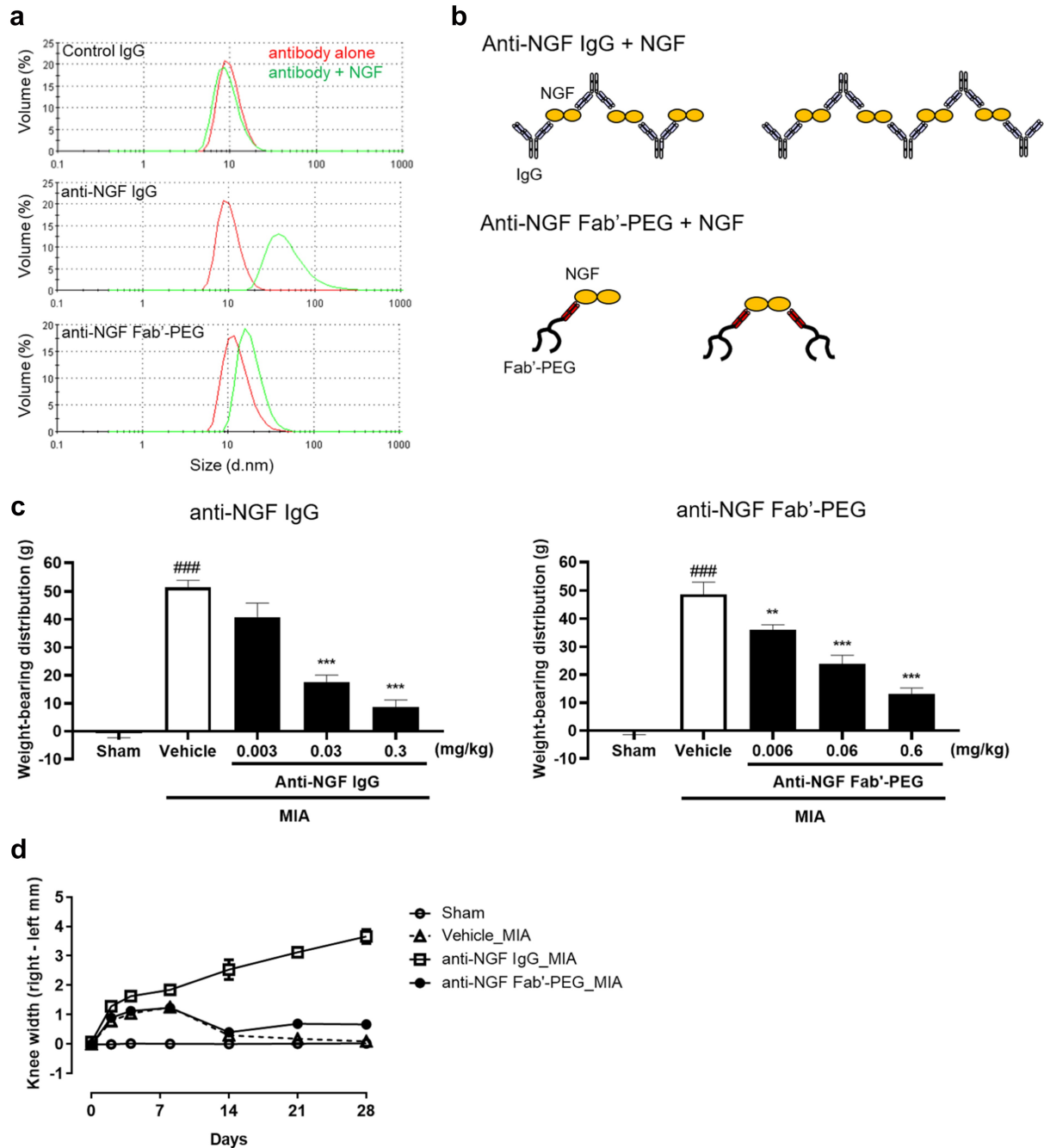

Figure 4. Comparison of the immune complex-forming ability and knee edema induced by anti-NGF Fab'-PEG and anti-NGF IgG in a rat MIA model. (a) DLS analysis was used to detect the particle size of the immune complex formed by control IgG, anti-NGF IgG and anti-NGF Fab'-PEG. The volume particle size distributions of complexes formed by antibody alone (red) or a mixture of antibody and NGF (green) were measured using Zetasizer Nano. (b) Difference in immune complex formation between the anti-NGF IgG and anti-NGF Fab'-PEG. (c) Analgesic effects of the anti-NGF IgG or Fab'-PEG determined via assessment of hind paw weight-bearing in MIA rats. Data are presented as mean ± SEM of 8 rats in each group. ### P < .001 statistically significant compared to the sham group (Student's t-test). ** P < .01 or *** P < .001, statistically significant compared to the vehicle group (Dunnett's multiple comparisons test). (d) Knee diameter was assessed in MIA model rats on day 0, 2, 4, 8, 14, 21 and 28 post MIA injection. Rats were injected with 1 mg of MIA or saline (Sham) into the right knee. Anti-NGF IgG or PBS (Vehicle) was intravenously administered once (on day 2), or anti-NGF Fab'-PEG was intravenously administered 4 times (on day 2, 10, 18 and 26) after MIA injection. Knee width was determined by subtracting the value for the left side from that for the right. Data are presented as the mean ± SEM of 6 rats in each group.

Table 2. Particle size of immune complexes.

	Volume-Particle size	
	Peak (d.nm)	Mean (d.nm)
Control IgG alone	8.7	10.2
Control IgG + NGF	8.7	9.5
anti-NGF IgG alone	8.7	10.3
anti-NGF IgG + NGF	37.8	52.9
anti-NGF Fab'-PEG alone	11.7	17.2
anti-NGF Fab'-PEG + NGF	15.7	23.2

DLS analysis was used to detect the particle size of the immune complexes. Peak and mean diameters (nm) based on volume particle size distributions (shown in Figure 4a) were measured using Zetasizer Nano.

37.8 nm after incubation with NGF. In contrast, for the control antibody, which does not bind to NGF, the peak diameter remained at 8.7 nm. Based on these findings, we considered the shift in particle diameter to be an indicator of the formation of an IC. In addition, the distribution of the size of anti-NGF IgG + NGF showed a tail on the high particle size side, and the average diameter changed significantly from 10.3 nm to 52.9 nm, suggesting that some large ICs also formed in solution. In contrast, in the case of anti-NGF Fab'-PEG, the peak diameter changed from 11.7 nm to 15.7 nm, a clearly much smaller shift than that observed for anti-NGF IgG. Since anti-NGF Fab'-PEG only has a monovalent antigen-binding site, it cannot form large ICs by crosslinking antigens or even if the antigen is a dimer (Figure 4b).

Next, we evaluated and compared the efficacy and safety of the anti-NGF Fab'-PEG and anti-NGF IgG in MIA-induced OA model rats. At 21 days after the MIA injection, the model rats (vehicle) showed an increase in weight-bearing distribution (mean ± SEM, 51.42 ± 2.63 g or 48.69 ± 4.41 g) compared to sham rats (−0.63 ± 1.72 g or −0.47 ± 0.94 g). Administration of anti-NGF IgG (17.61 ± 2.44 g for 0.03 mg/kg, 8.70 ± 2.48 g for 0.3 mg/kg) or anti-NGF Fab'-PEG (36.10 ± 1.68 g for 0.006 mg/kg, 23.91 ± 3.06 g for 0.06 mg/kg, 13.15 ± 2.07 g for 0.6 mg/kg) significantly decreased weight-bearing, suggesting that the antibodies improved pain behavior (Figure 4c). Findings on knee edema in the MIA model were particularly interesting. In MIA rats (vehicle) and the anti-NGF Fab'-PEG-administered group, the differences in knee diameter between the MIA-injected knee (right knee) and the contralateral knee (left knee) increased transiently before stabilizing after 14 days post MIA injection. In contrast, in the anti-NGF IgG-administered group, the knee diameter continued to increase over time. At 28 days post MIA injection, the knee diameter (mean ± SEM) in the anti-NGF IgG-administered group was 3.66 ± 0.24 mm, more than 5 times that measured in the anti-NGF Fab'-PEG-administered group (0.66 ± 0.095 mm) (Figure 4d). Magnetic resonance imaging of the MIA-injected knee at 28 days post MIA injection showed cartilage destruction at the distal femur and proximal tibia, and a similar degree of damage to that observed in anti-NGF Fab'-PEG-administered MIA rats (Figure S1). However, in the anti-NGF IgG-administered group, edema and damage to the cartilage and subchondral bone were observed in some individuals.

Discussion

We conjugated a branched 40 kDa PEG biocompatible polymer to the Fab' hinge region of an anti-NGF antibody to enhance the pharmacokinetics of the Fab'. This technique has been shown to prolong the in vivo half-lives of antibodies, possibly as a result of evasion of renal clearance because the polymer increases the apparent size of the molecule such that it is above the threshold for glomerular filtration.[25,34] To retain the high antigen binding affinity of the Fab', as reported for the PEGylated anti-TNF-α Fab' antibody certolizumab pegol, PEGylation was performed in a site-specific manner, at a position distant from the variable region of Fab', which binds NGF.[34] The anti-NGF Fab'-PEG exhibited high NGF binding affinity and in vitro NGF neutralizing activity comparable to that of the anti-NGF IgG. PEGylation offers several other important potential advantages, including improved thermal and mechanical stability, and solubility in aqueous solution. Since the anti-NGF Fab'-PEG was less likely to form aggregates than IgG when heated to 50°C, it may also have excellent stability beneficial for manufacture and storage.[35]

The results in CIA mice indicate that the anti-NGF Fab'-PEG penetrates inflamed arthritic paws more effectively than the IgG. Consistent with this, a previous study demonstrated that the anti-TNF-α Fab'-PEG certolizumab pegol was more effectively distributed into inflamed arthritic paws than anti-TNF-α IgG in CIA model mice.[33] In patients with rheumatoid arthritis and spondyloarthritis, certolizumab pegol showed statistically significant higher uptake in swollen joints compared to clinically negative joints.[36] While PEGylated proteins tend not to diffuse out of blood into normal tissues due to their associated water shell, the increase in vascular permeability enhances their diffusion into inflamed tissue.[37] Once the PEGylated Fab' diffuses into tissue, it might remain there for longer periods of time because the lack of an Fc region reduces recycling of the Fab' out of the tissue by FcRn. The pH in OA joints is lower, at around 6.0, than the physiological pH, which might promote binding of IgG to FcRn to facilitate recycling.[23,38] In addition, increased FcRn expression in the paws of CIA mice, according to preliminary data, may further facilitate the difference between Fab'-PEG and IgG. Given that NGF is upregulated at osteochondral junctions in patients with OA compared with non-arthritic controls, we believe that improved retention in inflammatory tissues may lead to enhanced drug efficacy in pathological conditions and reduced adverse effects in normal tissues.[8]

We also demonstrated a clear difference in the placental transfer efficiency between IgG and Fab'-PEG in rats and non-human primates (NHPs). In most mammalian species including humans, maternal IgG antibodies cross the placenta through pH-dependent binding to the neonatal Fc receptor, FcRn. However, there are known anatomic differences in placental/yolk sac structure among mammals. While the transfer of IgG from the maternal to fetal circulation occurs almost exclusively prenatally via the chorioallantoic placenta in humans and NHPs, it occurs both prenatally via the inverted yolk sac and postnatally in the milk in rodents.[20,21] Therefore, we examined placental transfer in both rats and NHPs. FcRn-mediated placental transfer of maternally derived IgGs has been shown to increase with gestational age.[39] In a previous study of placental transfer after administration of human IgG2 in late gestation, the fetal plasma concentration reached approximately 15% of the maternal plasma concentration in GD 16–21 rats, and approximately 5% in the second trimester (GD 50–70) in cynomolgus monkeys.[20] In the present study, the fetal plasma concentration was approximately 75% of the maternal plasma concentration in GD 20 rats, which is higher than that in the previous study, suggesting possible contamination of maternal plasma. In contrast, placental transfer in NHPs was similar to that in the previous study. It should be noted that, unlike IgG, Fab-PEG clearly did not show placental transfer, indicating a clear difference between the antibodies in postnatal development in rats. In the anti-NGF IgG-treated group, all pups exhibited attenuated response to pain and died before weaning with little or no milk in the stomach. Previous studies indicate that NGF is an essential factor in nerve development in the early stages of development. Studies in mice lacking NGF and rats producing anti-NGF antibodies have shown that depriving the fetus of NGF leads to the destruction of most dorsal root ganglion neurons and sympathetic neurons.[15,40] Additionally, mutant NGF knock-in mice and NGF-/-; Bax-/- mice display smaller milk spots in the stomach, indicating they could not ingest normal quantities of milk because of deficient feeding behavior.[41,42] This may be related to a sensory nervous system defect that affects mother-pup or pup-pup interactions. Our results showed similar abnormalities in the post-neonatal development of pups birthed from anti-NGF IgG-treated dams; notably, anti-NGF Fab-PEG led to normal development because it was not transferred through the placenta. Since NGF mutations cause congenital insensitivity, NGF is also clearly an essential factor for nerve development in humans.[13] Among the diseases related to NGF, OA and chronic low back pain affect mostly older patients, but migraine additionally affects many women of childbearing age.[43] Therefore, anti-NGF IgG may increase the risk of adverse effects on child development when administered to pregnant patients. Our results indicate that our anti-NGF Fab'-PEG might be a safer therapeutic antibody associated with lower risk of abnormal development.

Interestingly, we found that while the anti-NGF IgG exacerbated knee joint edema and damage to subchondral bone in MIA rats, our anti-NGF Fab'-PEG led to only transient and mild knee edema. Treatment with the anti-NGF IgG resulted in a statistically significant increase in knee edema size in MIA rats, a finding which is consistent with a previous report, which

suspected that the edema might be caused by an increase in weight-bearing distribution to the arthritic joint due to a reduction in pain.[29] However, the present data do not support this theory. Although our Fab'-PEG showed the same analgesic effect as the IgG, the influence on the degree of edema was clearly different. While the mechanism of this effect remains to be elucidated, our finding that IgG and Fab-PEG exhibited different IC-forming abilities (Figure 4a) leads us to hypothesize that excess ICs formed by IgG might accumulate in the knee joint where they trigger an immune response to cause edema. Usually, ICs are bound to a complement and transported to the liver and spleen by erythrocytes via binding to the complement receptor 1. They are then phagocytosed by monocytes, dendritic cells, macrophages, and hepatic Kupffer cells. However, the anti-NGF IgG used in the present study has an Fc variant of IgG2 engineered with A330S/P331S substitutions to eliminate affinity for the C1q complement protein while retaining FcγR binding and effector functions and, consequently, metabolism of ICs by erythrocytes.[44,45] Therefore, once ICs are formed in local tissues expressing NGF, they likely remain there. The Fc regions within ICs in tissues can then engage Fc receptors on neutrophils, basophils, lymphocytes and platelets to induce inflammation by releasing cytokines and increase vascular permeability by inducing vasoactive amine release.[46] Additionally, IgG2 ICs activate osteoclastogenesis by binding to FcγRI and FcγRIV, which is induced under inflammatory conditions.[47] This proposed mechanism is partially similar to that reported for the pathophysiology of inflammatory arthritis conditions such as rheumatoid arthritis.[48] Meta-analysis of randomized Phase 3 clinical trials indicates that tanezumab significantly increases the incidence of RPOA compared with placebo, although the potential mechanisms underlying the clinical findings of increased RPOA are largely unknown.[49,50] Given that tanezumab has the same Fc region sequence as we used in the present study, it might cause edema and damage to the joints of patients, as we observed in MIA rats.[45] Importantly, however, the anti-NGF Fab'-PEG did not exacerbate edema or have any adverse effects in MIA rats, suggesting that it could be an excellent therapeutic candidate for OA patients.

We also reported a novel and simple method for estimating the size of an antibody-antigen IC by measuring the particle size distribution obtained by DLS analysis. The difference in the size of ICs formed by IgG compared to Fab'-PEG in this study is thought to be caused by the difference in valence of the antibodies. However, differences in IC size can also occur between IgGs due to differences in the binding affinity or epitopes of individual IgGs. In previous reports, IC size was investigated using cation exchange and size exclusion liquid chromatography.[51,52] Compared to these techniques, the method used in this study is simpler and can be used to screen for therapeutic IgGs by using IC formation as an index. DLS might be useful for wider IC analysis as it has previously been used to analyze ICs formed by antibodies and anti-drug antibodies.[52] Our novel and simple method for analyzing IC size may make it easier to select safer therapeutic antibodies.

In conclusion, our anti-NGF Fab'-PEG showed strong analgesic effects with higher accumulation in the lesion site of OA models, undetectable placental transfer and induced

limited knee edema. These findings suggest that our anti-NGF Fab'-PEG might be a potential therapeutic candidate with lower risk of adverse effects for various diseases in which NGF is involved such as OA and chronic back pain. While this study reported only non-clinical study data, Phase 1 and Phase 2a clinical studies of anti-NGF Fab'-PEG (ASP6294) have been completed, and ASP6294 was well-tolerated and safe in healthy subjects and subjects with bladder pain syndrome/interstitial cystitis. Astellas has discontinued further development of ASP6294 for strategic reasons. However, based on the favorable safety profile in the clinical trial, we hope the potential of this therapeutic drug will continue to be investigated in other pain diseases in the future.

Materials and Methods

Ethics statement

All methods were performed in accordance with institutional guidelines approved by Astellas Pharma and relevant guidelines and regulations. All animal experiments were approved by the Institutional Animal Care and Use Committee (IACUC) of Astellas Pharma and performed in accordance with the guidelines of the Care and Use of Laboratory Animals at Astellas Pharma and in full compliance with the ARRIVE guidelines. Tsukuba Research Center was awarded Accreditation Status by the AAALAC International.

Animals

C57BL/6 J mice (male, 5 weeks old), Sprague Dawley rats (male, 5 weeks old), female 14-day pregnant Sprague Dawley rats and DBA/1 mice (male, 5 weeks old) were obtained from Charles River Japan. Virgin female Sprague Dawley rats (11–15 weeks old, Charles River Japan) were mated with males (11–17 weeks old, Charles River Japan) on a one-to-one basis in the male's cage overnight to obtain pregnant animals, and the day on which a vaginal plug was found or sperm was present in smears was designated GD 0. Female cynomolgus monkeys with regular menstrual cycles were mated with males of proven fertility for three consecutive days between the 11th and 15th days of each monkey's menstrual cycle at Shin Nippon Biomedical Laboratories, and the mid-point of the mating period was designated GD 0. Animals were housed under conditions that included a controlled light cycle (light/dark: 12 hours each) and controlled temperature. Animals were fed standard laboratory food and water, both of which were available ad libitum.

Cell culture

HEK293 cells stably expressing human TrkA were established at Astellas Pharma as described previously and cultured with DMEM including 10% fetal bovine serum (FBS), penicillin (100 units/mL), streptomycin (100 μg/mL) and 200 μg/mL G418 at 37°C with 5% CO_2.[29]

Immunization and screening of anti-NGF antibodies

Monoclonal antibodies against NGF were produced by immunizing VelocImmune mice (Regeneron), which are genetically modified to produce human antibodies. For immunization, a recombinant human NGF protein (R&D Systems) was injected into VelocImmune mice together with an adjuvant to induce an immune reaction. Using a standard method, the lymph nodes of the immunized mice were extracted, and lymphocytes were collected and cell-fused with mouse-derived myeloma cell SP2/0 to prepare a hybridoma. The hybridoma was cloned by limiting dilution and each clone was cultured in serum-free culture medium. IgG were purified from the culture supernatant using a Protein G or Protein A column. Fab fragments were prepared using a Fab preparation kit (Pierce). IgG was digested using immobilized papain protease and the Fab fraction was subsequently purified by removing Fc and intact IgG using a Protein G column.

Competitive ELISA

Competitive ELISA was performed using biotinylated NGF and recombinant TrkA protein. Briefly, human and mouse NGF were biotinylated using EZ-LINK 5-biotinamido pentylamide (Pierce) and mixed with an antibody solution. The mixture was added to a microplate immobilized with recombinant TrkA (R&D Systems). Alkaline phosphatase-labeled streptavidin followed by chemiluminescent AP substrate (Surmodics) were added and chemiluminescence was measured.

NGF/TrkA cell signal assay using Fluorescence Imaging Plate Reader (FLIPR)

HEK293 cells expressing human TrkA were seeded at 2×10^4 cells per well into black-walled, clear bottom 96-well poly-d-lysine-coated plates (BD Biosciences) and incubated overnight at 37°C. On the day of measurement, cells were incubated with DMEM containing 3.6 mmol/L sodium hydroxide, 2.5 mmol/L probenecid (Sigma) and the calcium indicator Fluo-4 AM (Dojindo) for 30 minutes at 37°C. After washing the cells, fresh Hank's Balanced Salt Solution (HBSS) containing 20 mM HEPES pH 7.4, 0.1% bovine serum albumin, 3.6 mmol/L sodium hydroxide, and 2.5 mmol/L probenecid was added, and the plate was placed into a FLIPR TETRA device (Molecular Devices). Test antibody was mixed with NGF (final concentration 100 ng/mL) and preincubated in a microplate and added to the cells via FLIPR TETRA. Changes in cell fluorescence activity after addition of antibody/NGF were monitored and calculated as the maximum – minimum fluorescence values.

TrkA phosphorylation assay

Human TrkA-expressing HEK293 cells were seeded at 1×10^4 cells/well into a microplate and incubated overnight. Antibody was serially diluted with phosphate buffered saline (PBS) and incubated with recombinant human NGF (R&D Systems) for 10 minutes. The mixture was added to the microplate and

incubated for 1 hour. Supernatants were subsequently aspirated, and the cells lysed with cell lysing buffer (Cell Signaling) including 1 mmol/L phenylmethylsulfonyl fluoride (Sigma). The lysates were harvested and added to 0.05% Tween20/PBS. Anti-human TrkA antibody (Enzo) was diluted with PBS and coated onto a microplate. The plate was blocked with blocking buffer and washed with Tris-buffered saline with 0.05% Tween (TBS-T). The cell lysate was added to the plate and incubated for 2 hours at 37°C, then the plate was washed with TBS-T. Rabbit anti-human phospho-TrkA IgG (Cell Signaling) was added and the lysate was incubated for 1 hour at 37°C before washing the plate with TBS-T. Goat anti-rabbit IgG (Fc) alkaline phosphatase conjugate (Promega) was added and the lysate was incubated for 30 minutes at 37°C, then the plate washed with TBS-T. Chemiluminescent AP substrate (Surmodics) was added and chemiluminescence was measured using a plate reader.

ELISA

Recombinant human NGF (R&D Systems), BDNF (GenWay Biotech), NT-3 (Peprotech) and NT-4 (Peprotech) were diluted with PBS and coated onto a microplate. The plate was blocked with 20% Blocking One (Nacalai Tesque) containing TBS-T. The anti-NGF Fab'-PEG was added and the plate was incubated at room temperature, and then washed with TBS-T. Goat anti-human kappa-HRP (Southern Biotech) secondary antibody was added and the plate was incubated at room temperature, and then washed with TBS-T. TMB + One-Step Substrate System (Dako) was added. When a color change was observed, sulfuric acid was added and the absorbance at 450 nm was measured using a plate reader.

Generation of a genetically and chemically engineered anti-NGF Fab'-PEG

The genes encoding the heavy and light chains of the anti-NGF antibody were cloned from a hybridoma. An amino acid mutation was introduced into the complementarity-determining region of the heavy chain to remove the N-linked sugar-chain glycosylation motif to improve the antibody's productivity and homogeneity in the manufacturing process. To construct an expression vector for the Fab' fragment, a gene encoding a signal sequence and a gene encoding the constant region of human Igγ1 up to Cys226 (EU index numbering) or the constant region of human Igγ1 up to Cys226 followed by two alanine residues (Ala-Ala) were linked to the 5' and 3' ends, respectively, of the gene encoding the heavy chain variable region, and the heavy-chain gene was inserted into a GS® vector pEE6.4 (Lonza).[53] Further, a gene encoding a signal sequence and a gene encoding the constant region of the human kappa chain were connected to the 5' and 3' ends, respectively, of the gene encoding the light chain variable region, and the light-chain gene was inserted into a GS® vector pEE12.4 (Lonza). The GS® vectors into which the genes of the heavy and light chains of the antibody had each been inserted were digested with restriction enzymes NotI and PvuI and ligated into a single vector. To express the antibodies, expression vectors were transfected into FreeStyle 293 cells (Thermo) or CHOK1SV®

cells (Lonza). Antibodies were purified from each of the culture supernatants using KappaSelect (GE Healthcare).

To introduce PEG into the Fab', the Fab' fragment was reduced using 1 mmol/L Tris (2-carboxyethyl) phosphine hydrochloride (TCEP HCl) in 20 mM sodium phosphate buffer (pH 6.8) for 2 hours at 37°C, and then diluted with 20 mmol/L sodium acetate buffer (pH 5.0). This solution was adsorbed onto a cation exchange resin and eluted using a NaCl gradient solution. The obtained Fab' fragment was diluted with 20 mmol/L sodium phosphate buffer (pH 6.8) and left overnight or longer at 4°C to naturally oxidize. PEG of size 40 kDa (SUNBRIGHT GL2-400 MA, NOF Corporation) was added and the solution was incubated for 2 hours at room temperature followed by overnight at 4°C. The solution was diluted with 20 mmol/L sodium acetate buffer (pH 4.5) and adsorbed again onto a cation exchange resin and eluted using a NaCl gradient solution to purify the PEGylated Fab' fragment. The weights reported here include the weights of both the protein (Fab') and PEG.

Generation of anti-NGF IgG

The anti-NGF IgG was designed to have variable region sequences as reported previously and constant region sequences of IgG2 engineered with an A330S/P331S heavy chain and kappa light chain. IgG was stably expressed in CHOK1SV® cells (Lonza) using GS® vectors pEE12.4 and pEE6.4 (Lonza) and purified from the culture supernatant.[29]

Pharmacokinetics in mice

C57BL/6 J mice (Charles River, Japan) were intravenously administered anti-NGF Fab'-PEG (0.2 mg/kg) or anti-NGF IgG (0.3 mg/kg). Plasma samples were obtained 5 minutes and 1, 2, 6 and 24 hours after administration. The antibody concentration was measured in the same way as that described for the placental transfer study in rats.

Analgesic effect on an adjuvant-induced arthritis model

The AIA model has been well validated as an animal model of inflammatory pain. The number of rearing events has been evaluated as an objective indicator of pain in some animal models.[54, 55] C57BL/6 J mice (Charles River, Japan) were grouped in such a way as to minimize differences in average body weight among the groups the day before induction of arthritis. Test antibody or vehicle was intravenously administered, and 25 μL of Complete Freund's Adjuvant (Sigma) was immediately injected into both footpads of mice. In the sham group, saline was injected instead of Complete Freund's Adjuvant. Approximately 24 hours later, the degree of inflammatory pain was assessed by measuring the number of rearing events, which were automatically counted for 20 minutes using SUPERMEX model MRS-110 (Muromachi Kikai).[55]

Distribution into lesioned tissue in collagen-induced arthritis model

DBA/1 mice were subcutaneously administered an emulsion including collagen (bovine joint-derived type 2 collagen,

10 mg/mL; Collagen Technique Workshop) and Complete Freund's Adjuvant (0.5 mg/mL; DIFCO) at a ratio of 1:1 into the ankle joint. Four weeks later, the emulsion was administered again to cause arthritis. Mice were grouped in such a way as to minimize differences in the degree of arthritis (score and size of swelling). The test antibody was fluorescently labeled using the SAIV Rapid Antibody Labeling Kit, Alexa Fluor 680 (Life Technologies) and intravenously administered into the tail vein at 2 mg/kg. The fluorescence intensity in the swollen footpad was analyzed for 50 hours from an hour after administration using IVIS Spectrum (Caliper/Xenogen).

Placental transfer of antibody in rats

The test antibody was intravenously administered at 10 mg/kg to three female Sprague-Dawley rats on the 17th day of pregnancy. Three days later, the antibody concentration in the blood of mothers and fetuses were measured in the following manner. After human NGF (R&D Systems) was added to a Multi-Array standard 96-well plate (Meso Scale Discovery) and immobilized, the plate was washed with TBST. The blocking agent (Blocker Casein in TBS; Thermo Fisher Scientific) was added and the plate was incubated at room temperature, and then washed with TBST. A blood sample was added, and the plate was incubated, and then washed with TBST. Biotin-labeled anti-human Kappa antibody (Immuno-Biological Laboratories) was added, and the plate was incubated, and then washed with TBST. SULFO-TAG-labeled streptavidin (Meso Scale Discovery) was added, and the plate was incubated, and then washed with TBST. Read Buffer T (Meso Scale Discovery) was added, and the amount of electrochemical luminescence was measured using SECTOR Imager 6000 (Meso Scale Discovery).

Effects on dams and embryo-fetal and postnatal development

Groups of 5–6 pregnant female rats were intravenously administered anti-NGF Fab'-PEG (3, 10 and 30 mg/kg once every other day from GD 7 to 19), anti-NGF IgG (10, 30 and 100 mg/kg twice on GD 7 and 14) or PBS alone. The highest dose was defined as the highest dose technically possible based on the solubility of the formulation, and the middle and low doses were selected to confirm the correlation with dose. The dams were allowed to deliver spontaneously. Items observed in dams included general signs, body weight, body weight gain, food consumption, delivery observations, gestation period, gestation index, nursing behavior, and gross pathology (including the number of implantations). To determine the plasma concentration of the test antibody and the presence of anti-drug antibodies, satellite groups consisting of three pregnant females/group were included. Items observed in pups included general signs, suckling ability, body weight, body weight gain, external abnormalities, macroscopic eye conditions, pain response, live birth index, viability index, weaning index, and gross pathology (visceral abnormalities).

Placental transfer of antibody in NHPs

Pregnant cynomolgus monkeys were intravenously administered anti-NGF Fab'-PEG (10 mg/kg) or anti-NGF IgG (10 mg/kg) on GD 49, 99 or 139. Serum samples were obtained from dams and fetuses the following day (GD 50, 100, or 140) to investigate placental transfer. Serum was taken from two pregnant cynomolgus monkeys on each sampling day. The antibody concentration was measured in the same way as that described for the placental transfer study in rats.

Formation of ICs

The test antibody was prepared to a concentration of 1 mg/ml (IgG) or 0.63 mg/mL (Fab'-PEG) and mixed with recombinant human NGF (R&D Systems) at a molar ratio of 1:1, and then incubated at room temperature for 3 hours to facilitate the formation of an IC. The incubated solution was transferred to a plastic cell (ZEN0040 Dispo micro cuvette 40 μL) and set and equilibrated at 25°C for 2 minutes in a Zetasizer Nano (Malvern). The size of the IC (diameter, nm) in the solution was determined by the volume or intensity distribution obtained from DLS and analyzed using Zetasizer v6.01 (Malvern).

Analgesic effect and knee edema in the MIA-induced arthritic model

Sprague-Dawley rats were anesthetized with 3–4% isoflurane (Mylan). The right knee was shaved and disinfected with 70% ethanol before injecting sodium MIA (Sigma) saline into the joint cavity at a dose of 1 mg in 50 μL via the patellar ligament, as described previously.[29,56] The sham group was injected with sterile isotonic saline without MIA. To evaluate the analgesic effect of the antibodies, anti-NGF IgG (0.003, 0.03, or 0.3 mg/kg) was intravenously administered 14 days after MIA injection, or anti-NGF Fab'-PEG (0.006, 0.06 or 0.6 mg/kg) was intravenously administered 18 and 20 days after MIA injection. Weight-bearing was evaluated at 21 days after MIA injection using an incapacitance meter (Linton Instruments) and used as an index of joint discomfort, as described previously.[56] Briefly, rats were placed in an angled plastic chamber positioned so that each hind paw rested on a separate force plate and were allowed to acclimate for about 5 minutes. The weight (g) measured for each hind paw was averaged for 5 seconds. The change in hind paw weight-bearing distribution was calculated by determining the difference in the weight between the left (contralateral control) and right (osteoarthritic) limbs. To evaluate the effect on knee edema, anti-NGF IgG (1 mg/kg) or PBS (vehicle group) was intravenously administered once 2 days after MIA injection, or anti-NGF Fab'-PEG (2 mg/kg) was intravenously administered 4 times 2, 10, 18 and 26 days after MIA injection. Knee diameter was measured using calibrated digital calipers, and differences in diameter between the right and left knee were determined by subtracting the value for the left side from that for the right (MIA-injected side), as described previously.[29]

At 28 days after MIA injection, rats were sacrificed and fixed with formalin. Proton magnetic resonance imaging (MRI)

data were acquired on a compact 1.5-Tesla MRI system (MRmini SA; DS Pharma Biomedical, Suita, Japan) with a 17 mm inner diameter solenoid coil. 3D-T1W images were obtained using a spin-echo sequence with the following parameters: pulse repetition time = 150 ms, echo time = 12 ms, matrix size = $256 \times 128 \times 64$, field of view = 15.2 mm, number of acquisitions = 8 and acquisition time for one set = 167 minutes. Image reconstruction and analysis were performed using an NMR Imager (MR Technology) and ImageJ (Ver. 1.x, NIH).

Statistical analyses

Data are presented as mean ± SD or mean ± SEM. Significant differences between the test and vehicle groups were determined using Student's t-test or Dunnett's multiple comparisons test in GraphPad Prism version 8.0.2 or 8.3.1. $P < .05$ was considered statistically significant.

Abbreviations

AIA	adjuvant-induced arthritis
BDNF	brain-derived neurotrophic factor
CIA	collagen-induced arthritis
DLS	dynamic light scattering
FBS	fetal bovine serum
FLIPR	fluorescent imaging plate reader
GD	gestational day
IACUC	Institutional Animal Care and Use Committee
IC	immune complex
K_D	dissociation constant
MIA	monoiodoacetate
NGF	nerve growth factor
NHP	non-human primate
NT-3	neurotrophin-3
NT-4	neurotrophin-4
OA	osteoarthritis
PBS	phosphate buffered saline
RPOA	rapidly progressive osteoarthritis
TNF	tumor necrosis factor
TrkA	tyrosine kinase receptor tropomyosin receptor kinase A

Author contributions

Y.K. contributed to the acquisition, analysis and interpretation of data, and main writing of the manuscript; H.T., E.Y and N.T. contributed to the conception or design of the study, and the acquisition, analysis, and interpretation of data; S.M., H.M, H.F. and K.M contributed to the acquisition, analysis, and interpretation of data; M.K. contributed to the conception or design of the study; all authors contributed to drafting and revising the manuscript and approved the final version.

Disclosure statement

This research was funded by Astellas Pharma. The authors are all employees of Astellas Pharma. Astellas Pharma holds patents (PCT/JP2012/070433) on the anti-human NGF antibody. Y.K., M.K, H.T., and E.Y. are inventors on the patent.

ORCID

Yukari Koya 🆔 http://orcid.org/0000-0003-3103-7271

References

1. Glyn-Jones S, Palmer AJ, Agricola R, Price AJ, Vincent TL, Weinans H, Carr AJ. Osteoarthritis. Lancet. 2015;386 (9991):376–87. PMID: 25748615. doi:10.1016/s0140-6736(14) 60802-3.
2. Dillon CF, Rasch EK, Gu Q, Hirsch R. Prevalence of knee osteoarthritis in the United States: arthritis data from the third national health and nutrition examination survey 1991-94. J Rheumatol. 2006;33(11):2271–79. PMID: 17013996
3. Kidd BL, Langford RM, Wodehouse T. Arthritis and pain. Current approaches in the treatment of arthritic pain. Arthritis Res Ther. 2007;9(3):214–214. PMID: 17572915. doi:10.1186/ar2147.
4. Hochman JR, French MR, Bermingham SL, Hawker GA. The nerve of osteoarthritis pain. Arthritis Care Res (Hoboken). 2010;62 (7):1019–23. PMID: 20589688. doi:10.1002/acr.20142.
5. Levi-Montalcini R. The nerve growth factor 35 years later. Science. 1987;237(4819):1154–62. PMID: 3306916. doi:10.1126/science. 3306916.
6. Hefti FF, Rosenthal A, Walicke PA, Wyatt S, Vergara G, Shelton DL, Davies AM. Novel class of pain drugs based on antagonism of NGF. Trends Pharmacol Sci. 2006;27(2):85–91. PMID: 16376998. doi:10.1016/j.tips.2005.12.001.
7. Mantyh PW, Koltzenburg M, Mendell LM, Tive L, Shelton DL, Warner DS. Antagonism of nerve growth factor-TrkA signaling and the relief of pain. Anesthesiology. 2011;115(1):189–204. PMID: 21602663. doi:10.1097/ALN.0b013e31821b1ac5.
8. Walsh DA, McWilliams DF, Turley MJ, Dixon MR, Fransès RE, Mapp PI, Wilson D. Angiogenesis and nerve growth factor at the osteochondral junction in rheumatoid arthritis and osteoarthritis. Rheumatology (Oxford). 2010;49(10):1852–61. PMID: 20581375. doi:10.1093/rheumatology/keq188.
9. Watson JJ, Allen SJ, Dawbarn D. Targeting nerve growth factor in pain: what is the therapeutic potential? BioDrugs. 2008;22 (6):349–59. PMID: 18998753. doi:10.2165/0063030-200822060- 00002.
10. Bradshaw RA, Murray-Rust J, Ibáñez CF, McDonald NQ, Lapatto R, Blundell TL. Nerve growth factor: structure/function relationships. Protein Sci. 1994;3(11):1901–13. PMID: 7703837. doi:10.1002/pro.5560031102.
11. Sánchez-Robles EM, Girón R, Paniagua N, Rodríguez-Rivera C, Pascual D, Goicoechea C. Monoclonal antibodies for chronic pain treatment: present and future. Int J Mol Sci. 2021;23(1):22. doi:10. 3390/ijms221910325.
12. Indo Y, Tsuruta M, Hayashida Y, Karim MA, Ohta K, Kawano T, Mitsubuchi H, Tonoki H, Awaya Y, Matsuda I. Mutations in the TRKA/NGF receptor gene in patients with congenital insensitivity to pain with anhidrosis. Nat Genet. 1996;13(4):485–88. PMID: 8696348. doi:10.1038/ng0896-485.
13. Einarsdottir E, Carlsson A, Minde J, Toolanen G, Svensson O, Solders G, Holmgren G, Holmberg D, Holmberg M. A mutation in the nerve growth factor beta gene (NGFB) causes loss of pain perception. Hum Mol Genet. 2004;13(8):799–805. PMID: 14976160. doi:10.1093/hmg/ddh096.
14. Smeyne RJ, Klein R, Schnapp A, Long LK, Bryant S, Lewin A, Lira SA, Barbacid M. Severe sensory and sympathetic neuropathies

in mice carrying a disrupted Trk/NGF receptor gene. Nature. 1994;368(6468):246–49. PMID: 8145823. doi:10.1038/368246a0.

15. Crowley C, Spencer SD, Nishimura MC, Chen KS, Pitts-Meek S, Armanini MP, Ling LH, McMahon SB, Shelton DL, Levinson AD, et al. Mice lacking nerve growth factor display perinatal loss of sensory and sympathetic neurons yet develop basal forebrain cholinergic neurons. Cell. 1994;76(6):1001–11. PMID: 8137419.

16. Manchikanti L, Cash KA, McManus CD, Pampati V, Benyamin RM. Preliminary results of a randomized, doubleblind, controlled trial of fluoroscopic lumbar interlaminar epidural injections in managing chronic lumbar discogenic pain without disc herniation or radiculitis. Pain Physician. 2010;13(4;7):E279–292. PMID: 20648214. doi:10.36076/ppj.2010/13/E279.

17. Wilkens P, Scheel IB, Grundnes O, Hellum C, Storheim K. Effect of glucosamine on pain-related disability in patients with chronic low back pain and degenerative lumbar osteoarthritis: a randomized controlled trial. Jama. 2010;304(1):45–52. PMID: 20606148. doi:10.1001/jama.2010.893.

18. Buynak R, Shapiro DY, Okamoto A, Van Hove I, Rauschkolb C, Steup A, Lange B, Lange C, Etropolski M. Efficacy and safety of tapentadol extended release for the management of chronic low back pain: results of a prospective, randomized, double-blind, placebo- and active-controlled Phase III study. Expert Opin Pharmacother. 2010;11(11):1787–804. PMID: 20578811. doi:10.1517/14656566.2010.497720.

19. Schnitzer TJ, Easton R, Pang S, Levinson DJ, Pixton G, Viktrup L, Davignon I, Brown MT, West CR, Verburg KM. Effect of tanezumab on joint pain, physical function, and patient global assessment of osteoarthritis among patients with osteoarthritis of the hip or knee: a randomized clinical trial. Jama. 2019;322(1):37–48. PMID: 31265100. doi:10.1001/jama.2019.8044.

20. Moffat GJ, Retter MW, Kwon G, Loomis M, Hock MB, Hall C, Bussiere J, Lewis EM, Chellman GJ. Placental transfer of a fully human IgG2 monoclonal antibody in the cynomolgus monkey, rat, and rabbit: a comparative assessment from during organogenesis to late gestation. Birth Defects Res B Dev Reprod Toxicol. 2014;101 (2):178–88. PMID: 24753333. doi:10.1002/bdrb.21105.

21. Bowman CJ, Breslin WJ, Connor AV, Martin PL, Moffat GJ, Sivaraman L, Tornesi MB, Chivers S. Placental transfer of Fc-containing biopharmaceuticals across species, an industry survey analysis. Birth Defects Res B Dev Reprod Toxicol. 2013;98 (6):459–85. PMID: 24391099. doi:10.1002/bdrb.21089.

22. Pasut G. Pegylation of biological molecules and potential benefits: pharmacological properties of certolizumab pegol. BioDrugs. 2014;28(Suppl 1):S15–23. PMID: 24687235. doi:10.1007/s40259-013-0064-z.

23. Roopenian DC, Akilesh S. FcRn: the neonatal Fc receptor comes of age. Nat Rev Immunol. 2007;7(9):715–25. doi:10.1038/nri2155.

24. Hamidi M, Azadi A, Rafiei P. Pharmacokinetic consequences of pegylation. Drug Deliv. 2006;13(6):399–409. PMID: 17002967. doi:10.1080/10717540600814402.

25. Chapman AP. PEGylated antibodies and antibody fragments for improved therapy: a review. Adv Drug Deliv Rev. 2002;54 (4):531–45. PMID: 12052713. doi:10.1016/s0169-409x(02) 00026-1.

26. Nesbitt AM, Brown DT, Stephens S, Foulkes R. Placental transfer and accumulation in milk of the anti-TNF antibody TN3 in rats: immunoglobulin G1 versus PEGylated Fab': 1119. Official J Am Coll Gastroenterol. | ACG. 2006;101:S438. doi:10.14309/00000434-200609001-01119.

27. Meyer T, Robles-Carrillo L, Robson T, Langer F, Desai H, Davila M, Amaya M, Francis JL, Amirkhosravi A. Bevacizumab immune complexes activate platelets and induce thrombosis in FCGR2A transgenic mice. J Thromb Haemost. 2009;7:171–81. PMID: 18983497. doi:10.1111/j.1538-7836.2008.03212.x.

28. Scappaticci FA, Skillings JR, Holden SN, Gerber HP, Miller K, Kabbinavar F, Bergsland E, Ngai J, Holmgren E, Wang J, et al. Arterial thromboembolic events in patients with metastatic carcinoma treated with chemotherapy and bevacizumab. J Natl Cancer Inst. 2007;99(16):1232–39. PMID: 17686822.

29. Ishikawa G, Koya Y, Tanaka H, Nagakura Y. Long-term analgesic effect of a single dose of anti-NGF antibody on pain during motion without notable suppression of joint edema and lesion in a rat model of osteoarthritis. Osteoarthritis Cartilage. 2015;23 (6):925–32. PMID: 25677108. doi:10.1016/j.joca.2015.02.002.

30. Sakurai Y, Fujita M, Kawasaki S, Sanaki T, Yoshioka T, Higashino K, Tofukuji S, Yoneda S, Takahashi T, Koda K, et al. Contribution of synovial macrophages to rat advanced osteoarthritis pain resistant to cyclooxygenase inhibitors. Pain. 2019;160 (4):895–907. PMID: 30585984.

31. Xu L, Nwosu LN, Burston JJ, Millns PJ, Sagar DR, Mapp PI, Meesawatsom P, Li L, Bennett AJ, Walsh DA, et al. The anti-NGF antibody muMab 911 both prevents and reverses pain behaviour and subchondral osteoclast numbers in a rat model of osteoarthritis pain. Osteoarthritis Cartilage. 2016;24(9):1587–95. PMID: 27208420.

32. Salimi-Moosavi H, Rathanaswami P, Rajendran S, Toupikov M, Hill J. Rapid affinity measurement of protein-protein interactions in a microfluidic platform. Anal Biochem. 2012;426(2):134–41. PMID: 22542978. doi:10.1016/j.ab.2012.04.023.

33. Palframan R, Airey M, Moore A, Vugler A, Nesbitt A. Use of biofluorescence imaging to compare the distribution of certolizumab pegol, Adalimumab, and infliximab in the inflamed paws of mice with collagen-induced arthritis. J Immunol Methods. 2009;348(1–2):36–41. PMID: 19567252. doi:10.1016/j.jim.2009.06.009.

34. Weir N, Athwal D, Brown D, Foulkes R, Kollias G, Nesbitt A, Popplewell A, Spitali M, Stephens S. A new generation of high-affinity humanized PEGylated Fab [acute accent] fragment anti-tumor necrosis factor-[alpha] monoclonal antibodies. Therapy. 2006;3:535–45. accessed 27 Aug 2022. https://link.gale.com/apps/doc/A225319483/AONE?u=anon~27138985&sid=googleScholar&xid=3ac3c5e0.

35. Masazumi K, Hirotsugu T, Yukari K, Jun T, Atsuo Y, Yoshimi E. inventors; Astellas Pharma, assignee. Novel anti-human NGF antibody. WO/2013/022083. 2013 Feb 14.

36. Lambert B, Carron P, D'Asseler Y, Bacher K, Van den Bosch F, Elewaut D, Verbruggen G, Beyaert R, Dumolyn C, De Vos F. (99m) Tc-labelled S-HYNIC certolizumab pegol in rheumatoid arthritis and spondyloarthritis patients: a biodistribution and dosimetry study. EJNMMI Res. 2016;6(1):88. PMID: 27957720. doi:10.1186/s13550-016-0245-0.

37. Veronese FM, Pasut G. PEGylation, successful approach to drug delivery. Drug Discov Today. 2005;10(21):1451–58. PMID: 16243265. doi:10.1016/s1359-6446(05)03575-0.

38. Konttinen YT, Mandelin J, Li TF, Salo J, Lassus J, Liljeström M, Hukkanen M, Takagi M, Virtanen I, Santavirta S. Acidic cysteine endoproteinase cathepsin K in the degeneration of the superficial articular hyaline cartilage in osteoarthritis. Arthritis Rheum. 2002;46(4):953–60. PMID: 11953972. doi:10.1002/art.10185.

39. Pentsuk N, van der Laan JW. An interspecies comparison of placental antibody transfer: new insights into developmental toxicity testing of monoclonal antibodies. Birth Defects Res B Dev Reprod Toxicol. 2009;86(4):328–44. PMID: 19626656. doi:10.1002/bdrb.20201.

40. Johnson EM Jr., Gorin PD, Brandeis LD, Pearson J. Dorsal root ganglion neurons are destroyed by exposure in utero to maternal antibody to nerve growth factor. Science. 1980;210(4472):916–18. PMID: 7192014. doi:10.1126/science.7192014.

41. Yang W, Sung K, Zhou F, Xu W, Rissman RA, Ding J, Wu C. Targeted mutation (R100W) of the gene encoding NGF leads to deficits in the peripheral sensory nervous system. Front Aging Neurosci. 2018;10:373. PMID: 30524266. doi:10.3389/fnagi.2018.00373.

42. Glebova NO, Ginty DD. Heterogeneous requirement of NGF for sympathetic target innervation in vivo. J Neurosci. 2004;24 (3):743–51. PMID: 14736860. doi:10.1523/jneurosci.4523-03.2004.

43. Sakai F, Igarashi H. Prevalence of migraine in Japan: a nationwide survey. Cephalalgia. 1997;17(1):15–22. PMID: 9051330. doi:10.1046/j.1468-2982.1997.1701015.x.

44. Vafa O, Gilliland GL, Brezski RJ, Strake B, Wilkinson T, Lacy ER, Scallon B, Teplyakov A, Malia TJ, Strohl WR. An engineered Fc variant of an IgG eliminates all immune effector functions via structural perturbations. Methods. 2014;65(1):114–26. PMID: 23872058. doi:10.1016/j.ymeth.2013.06.035.

45. Wilkinson I, Anderson S, Fry J, Julien LA, Neville D, Qureshi O, Watts G, Hale G, Karagiannis SN. Fc-engineered antibodies with immune effector functions completely abolished. PLOS One. 2021;16 (12):e0260954. PMID: 34932587. doi:10.1371/journal.pone.0260954.

46. Chen B, Vousden KA, Naiman B, Turman S, Sun H, Wang S, Vinall LMK, Kemp BP, Kasturiangan S, Rees DG, et al. Humanised effector-null FcγRIIA antibody inhibits immune complex-mediated proinflammatory responses. Ann Rheum Dis. 2019;78(2):228–37. PMID: 30459279.

47. Negishi-Koga T, Gober HJ, Sumiya E, Komatsu N, Okamoto K, Sawa S, Suematsu A, Suda T, Sato K, Takai T, et al. Immune complexes regulate bone metabolism through FcRγ signalling. Nat Commun. 2015;6(1):6637. PMID: 25824719.

48. Chang MH, Nigrovic PA. Antibody-dependent and -independent mechanisms of inflammatory arthritis. JCI Insight. 2019;4(5). PMID: 30843881. doi:10.1172/jci.insight.125278.

49. Yu Y, Lu ST, Sun JP, Zhou W. Safety of low-dose tanezumab in the treatment of hip or knee osteoarthritis: a systemic review and meta-analysis of randomized phase iii clinical trials. Pain Med. 2021;22(3):585–95. PMID: 33141224. doi:10.1093/pm/pnaa260.

50. LaBranche TP, Bendele AM, Omura BC, Gropp KE, Hurst SI, Bagi CM, Cummings TR, Grantham LE 2nd, Shelton DL, Zorbas MA. Nerve growth factor inhibition with tanezumab influences weight-bearing and subsequent cartilage damage in the rat medial meniscal tear model. Ann Rheum Dis. 2017;76(1):295–302. PMID: 27381034. doi:10.1136/annrheumdis-2015-208913.

51. Santora LC, Kaymakcalan Z, Sakorafas P, Krull IS, Grant K. Characterization of noncovalent complexes of recombinant human monoclonal antibody and antigen using cation exchange, size exclusion chromatography, and BIAcore. Anal Biochem. 2001;299(2):119–29. PMID: 11730333. doi:10.1006/abio.2001. 5380.

52. Tada M, Suzuki T, Ishii-Watabe A. Development and characterization of an anti-rituximab monoclonal antibody panel. MAbs. 2018;10(3):370–79. PMID: 29309213. doi:10.1080/19420862.2018. 1424610.

53. Co MS, Avdalovic NM, Caron PC, Avdalovic MV, Scheinberg DA, Queen C. Chimeric and humanized antibodies with specificity for the CD33 antigen. J Immunol. 1992;148(4):1149–54. PMID: 1737932

54. Buvanendran A, Kroin JS, Kari MR, Tuman KJ. A new knee surgery model in rats to evaluate functional measures of postoperative pain. Anesth Analg. 2008;107(1):300–08. PMID: 18635501. doi:10.1213/ane.0b013e3181732f21.

55. Matson DJ, Broom DC, Carson SR, Baldassari J, Kehne J, Cortright DN. Inflammation-induced reduction of spontaneous activity by adjuvant: a novel model to study the effect of analgesics in rats. J Pharmacol Exp Ther. 2007;320(1):194–201. PMID: 17050782. doi:10.1124/jpet.106.109736.

56. Takeshita N, Yoshimi E, Hatori C, Kumakura F, Seki N, Shimizu Y. Alleviating effects of AS1892802, a Rho kinase inhibitor, on osteoarthritic disorders in rodents. J Pharmacol Sci. 2011;115 (4):481–89. PMID: 21325780. doi:10.1254/jphs.10319fp.